Supplementary Material for "Integrating eco-evolutionary dynamics and modern coexistence theory"

Last revision: July 1, 2022

Contents

Appendix S1: Eco-evolutionary niche and competitive ability differences

We show the derivation of the eco-evolutionary niche and competitive ability differences in

Equations 4-5 in the main text (with all parameters defined in the main text):

$$ND_{EE} = \frac{ND|_i + ND|_j}{2} + \frac{FD|_j - FD|_i}{2},$$ (S1.1)

and

$$FD_{EE} = \frac{FD|_i + FD|_j}{2} + \frac{ND|_j - ND|_i}{2}.$$ (S1.2)

The eco-evolutionary niche difference, ND_{EE}, can be written as:

$$
\begin{aligned}
-\ln\left(\rho_{EE}\right) &= -\ln\left(\sqrt{\dfrac{\alpha_{ji}\big|_i\,\alpha_{ij}\big|_j}{\alpha_{ii}\big|_i\,\alpha_{jj}\big|_j}}\right) \\[2mm]
&= -\ln\left[\sqrt{\sqrt{\dfrac{\left(\alpha_{ji}\big|_i\right)^2}{\left(\alpha_{ii}\big|_i\right)^2}}}\,\sqrt{\sqrt{\dfrac{\left(\alpha_{ij}\big|_j\right)^2}{\left(\alpha_{jj}\big|_j\right)^2}}}\right] \\[2mm]
&= -\ln\left(\sqrt{\sqrt{\dfrac{\alpha_{ji}\big|_i\,\alpha_{ij}\big|_i}{\alpha_{ii}\big|_i\,\alpha_{jj}\big|_i}}\,\sqrt{\dfrac{\alpha_{jj}\big|_i\,\alpha_{ji}\big|_i}{\alpha_{ii}\big|_i\,\alpha_{ij}\big|_i}}}\,\sqrt{\sqrt{\dfrac{\alpha_{ji}\big|_j\,\alpha_{ij}\big|_j}{\alpha_{ii}\big|_j\,\alpha_{jj}\big|_j}}\,\sqrt{\dfrac{\alpha_{ii}\big|_j\,\alpha_{ij}\big|_j}{\alpha_{jj}\big|_j\,\alpha_{ji}\big|_j}}}\right) \\[2mm]
&= -\ln\left(\sqrt{\sqrt{\dfrac{\alpha_{ji}\big|_i\,\alpha_{ij}\big|_i}{\alpha_{ii}\big|_i\,\alpha_{jj}\big|_i}}\,\sqrt{\dfrac{\alpha_{ji}\big|_j\,\alpha_{ij}\big|_j}{\alpha_{ii}\big|_j\,\alpha_{jj}\big|_j}}}\,\sqrt{\sqrt{\dfrac{\alpha_{jj}\big|_i\,\alpha_{ji}\big|_i}{\alpha_{ii}\big|_i\,\alpha_{ij}\big|_i}}\Bigg/\sqrt{\dfrac{\alpha_{jj}\big|_j\,\alpha_{ji}\big|_j}{\alpha_{ii}\big|_j\,\alpha_{ij}\big|_j}}}\right) \\[2mm]
&= -\ln\left(\sqrt{\rho\big|_i\,\rho\big|_j}\,\sqrt{\dfrac{\kappa_i}{\kappa_j}\bigg|_i\Bigg/\dfrac{\kappa_i}{\kappa_j}\bigg|_j}\right) \\[2mm]
&= \dfrac{-\ln\left(\rho\big|_i\right)-\ln\left(\rho\big|_j\right)}{2}+\dfrac{\ln\left(\dfrac{\kappa_i}{\kappa_j}\bigg|_j\right)-\ln\left(\dfrac{\kappa_i}{\kappa_j}\bigg|_i\right)}{2} \qquad\qquad \text{(S1.3)} \\[2mm]
&= \dfrac{ND\big|_i+ND\big|_j}{2}+\dfrac{FD\big|_j-FD\big|_i}{2}.
\end{aligned}
$$

On the other hand, the eco-evolutionary competitive ability difference, FD_{EE}, can be written as:

$$\ln\left(\frac{\kappa_i}{\kappa_j}\bigg|_{EE}\right) = \ln\left(\sqrt{\frac{\alpha_{jj}\big|_j}{\alpha_{ii}\big|_i}\frac{\alpha_{ji}\big|_i}{\alpha_{ij}\big|_j}}\right)$$

$$= \ln\left[\sqrt{\sqrt{\frac{\left(\alpha_{ji}\big|_i\right)^2}{\left(\alpha_{ii}\big|_i\right)^2}}}\sqrt{\sqrt{\frac{\left(\alpha_{jj}\big|_j\right)^2}{\left(\alpha_{ij}\big|_j\right)^2}}}\right]$$

$$= \ln\left(\sqrt{\sqrt{\frac{\alpha_{jj}\big|_i\,\alpha_{ji}\big|_i}{\alpha_{ii}\big|_i\,\alpha_{ij}\big|_i}}\sqrt{\frac{\alpha_{ji}\big|_i\,\alpha_{ij}\big|_i}{\alpha_{ii}\big|_i\,\alpha_{jj}\big|_i}}}\sqrt{\sqrt{\frac{\alpha_{jj}\big|_j\,\alpha_{ji}\big|_j}{\alpha_{ii}\big|_j\,\alpha_{ij}\big|_j}}\sqrt{\frac{\alpha_{ii}\big|_j\,\alpha_{jj}\big|_j}{\alpha_{ji}\big|_j\,\alpha_{ij}\big|_j}}}\right)$$

$$= \ln\left(\sqrt{\sqrt{\frac{\alpha_{jj}\big|_i\,\alpha_{ji}\big|_i}{\alpha_{ii}\big|_i\,\alpha_{ij}\big|_i}}\sqrt{\frac{\alpha_{jj}\big|_j\,\alpha_{ji}\big|_j}{\alpha_{ii}\big|_j\,\alpha_{ij}\big|_j}}}\sqrt{\sqrt{\frac{\alpha_{ji}\big|_i\,\alpha_{ij}\big|_i}{\alpha_{ii}\big|_i\,\alpha_{jj}\big|_i}}\bigg/\sqrt{\frac{\alpha_{ji}\big|_j\,\alpha_{ij}\big|_j}{\alpha_{ii}\big|_j\,\alpha_{jj}\big|_j}}}\right)$$

$$= \ln\left(\sqrt{\frac{\kappa_i}{\kappa_j}\bigg|_i\,\frac{\kappa_i}{\kappa_j}\bigg|_j}\sqrt{\frac{\rho\big|_i}{\rho\big|_j}}\right)$$

$$= \frac{\ln\left(\frac{\kappa_i}{\kappa_j}\bigg|_j\right) + \ln\left(\frac{\kappa_i}{\kappa_j}\bigg|_i\right)}{2} + \frac{-\ln\left(\rho\big|_j\right) + \ln\left(\rho\big|_i\right)}{2} \tag{S1.4}$$

$$= \frac{FD\big|_i + FD\big|_j}{2} + \frac{ND\big|_j - ND\big|_i}{2}.$$

Appendix S2: Neighbor-dependent selection model in Vasseur et al. (2011)

We replicate Figure 5 of Vasseur et al. (2011), where they considered competition dynamics

between two species, f and v (1 and 2 in the main text):

$$\frac{dN_f}{dt} = r_f N_f \left[1 - \alpha_{ff} N_f - \bar{\alpha}_{fv}(\bar{x}) N_v \right],$$
$$\frac{dN_v}{dt} = r_v N_v \left[1 - \bar{\alpha}_{vf}(\bar{x}) N_f - \bar{\alpha}_{vv}(\bar{x}) N_v \right],$$

(S2.1)

where r_i is the intrinsic growth rate, α_{ij} is the intraspecific or interspecific competition

coefficient, N_i is the population density of species i ($i, j = f, v$), and x is the quantitative trait of

species v. The trait is assumed to be normally distributed with a mean value $\bar{x}$ and variance

σ^2, and competition coefficients is assumed to be represented by

$$\bar{\alpha}_{fv}(\bar{x}) = c_1 + \left(\frac{\tau}{\sqrt{\tau^2 + \sigma^2}} \right) \exp\left[\frac{-(\bar{x} - \theta_H)^2}{2\tau^2 + 2\sigma^2} \right],$$

$$\bar{\alpha}_{vf}(\bar{x}) = 1 + c_1 - \left(\frac{\tau}{\sqrt{\tau^2 + \sigma^2}} \right) \exp\left[\frac{-(\bar{x} - \theta_H)^2}{2\tau^2 + 2\sigma^2} \right],$$

(S2.2)

$$\bar{\alpha}_{vv}(\bar{x}) = 1 + c_1 - \delta - (1 - 2\delta) \left(\frac{\tau}{\sqrt{\tau^2 + \sigma^2}} \right) \exp\left[\frac{-(\bar{x} - \theta_C)^2}{2\tau^2 + 2\sigma^2} \right],$$

after an integration, where θ_H and θ_C are the optimal trait values when the environment is

dominated by heterospecifics and conspecifics, respectively, c_1 and δ are constants that

determine the extreme values and relative rate at which the competitive coefficients change

with the trait, respectively, and τ is the width of the Gaussian function (Fig. S1A). This

indicates that increasing $\bar{\alpha}_{vf}$ decreases $\bar{\alpha}_{vv}$ and $\bar{\alpha}_{fv}$. The trait changes according to the

fitness gradient (Abrams 2001),

$$\frac{d\bar{x}}{dt} = H\sigma^2 \frac{\partial}{\partial \bar{x}}\left(\frac{1}{N_v}\frac{dN_v}{dt}\right), \tag{S2.3}$$

where H is the heritability and $dN/dt/N$ represents the per-capita growth rate (fitness).

The realized niche and competitive ability differences can be represented by

$$\rho = \sqrt{\frac{\bar{\alpha}_{fv}(\bar{x})\bar{\alpha}_{vf}(\bar{x})}{\alpha_{ff}\bar{\alpha}_{vv}(\bar{x})}},$$
$$\frac{\kappa_f}{\kappa_v} = \sqrt{\frac{\bar{\alpha}_{vv}(\bar{x})\bar{\alpha}_{vf}(\bar{x})}{\alpha_{ff}\bar{\alpha}_{fv}(\bar{x})}}. \tag{S2.4}$$

On the other hand, the eco-evolutionary niche and competitive ability differences defined in the main text are:

$$\rho_{EE} = \sqrt{\frac{\bar{\alpha}_{vf}(\theta_H)\bar{\alpha}_{fv}(\theta_C)}{\alpha_{ff}\bar{\alpha}_{vv}(\theta_C)}},$$
$$\left.\frac{\kappa_f}{\kappa_v}\right|_{EE} = \sqrt{\frac{\bar{\alpha}_{vv}(\theta_C)\bar{\alpha}_{vf}(\theta_H)}{\alpha_{ff}\bar{\alpha}_{fv}(\theta_C)}}. \tag{S2.5}$$

When the eco-evolutionary dynamics shows cyclic dynamics (Fig. S1C-D), the eco-evolutionary niche and competitive ability differences indicates stable coexistence (the blue and orange points in Fig. S1B). When the dynamics converges to a stable equilibrium (Fig. S1E), the eco-evolutionary condition also implies stable coexistence (the black point in Fig. S1B).

Appendix S3: Quantitative trait coevolution model in Mougi (2013)

We replicate Figure 1a of Mougi (2013), where they modeled the eco-evolutionary dynamics

of competition between two species:

$$
\begin{aligned}
\frac{dN_i}{dt} &= N_i \left[r_i(u_i) - N_i - \alpha_{ij}(u_i - u_j) N_j \right], \\
\frac{du_i}{dt} &= G_i \frac{\partial}{\partial u_i} \left(\frac{1}{N_i} \frac{dN_i}{dt} \right),
\end{aligned}
\tag{S3.1}
$$

where r_i is the per-capita growth rate, α_{ij} is the interspecific competition coefficient, and G_i is

the additive genetic variance (i, j = 1, 2). The authors assumed the effects of the trait as

$$
\begin{aligned}
r_i(u_i) &= r_0 \left(1 - u_i^{\rho_i} \right), \\
\alpha_{ij}(u_i - u_j) &= \frac{\alpha_0}{1 + \exp\left[\theta(u_i - u_j) \right]},
\end{aligned}
\tag{S3.2}
$$

as shown in Fig. S2A-B, trait values do not become negative ($u_i > 0$), and the trait evolves

along the fitness gradient (Abrams 2001). The realized niche and competitive ability

differences can be represented by

$$
\begin{aligned}
\rho &= \sqrt{\alpha_{12}(u_1 - u_2)\alpha_{21}(u_2 - u_1)}, \\
\frac{\kappa_1}{\kappa_2} &= \frac{r_1(u_1)}{r_2(u_2)} \sqrt{\frac{\alpha_{21}(u_2 - u_1)}{\alpha_{12}(u_1 - u_2)}}.
\end{aligned}
\tag{S3.3}
$$

The simulation (Fig. S2C-D) is similar to that of the neighbor-dependent selection model

(Fig. S1) because there is a negative correlation between interspecific competition

coefficients. When there is no competitor, evolution favors smaller trait values and eventually

7

the trait goes to zero. In this situation, the invader's optimal trait can be obtained by solving $du_i/dt = 0$ when $u_j = 0$ and $N_j = r_j(0)$. By using these trait values, we can calculate the extreme conditions (the top and bottom black points in Fig. S2C).

When the dynamics are represented by

$$\frac{dN_i}{dt} = N_i \left(r_i - a_{ii} N_i - a_{ij} N_j \right), \tag{S3.4}$$

unlike the main text, the eco-evolutionary niche and competitive ability differences are:

$$\rho_{EE} = \sqrt{\left. \frac{r_i a_{ji}}{r_j a_{ii}} \right|_i \left. \frac{r_j a_{ij}}{r_i a_{jj}} \right|_j},$$

$$\frac{\kappa_1}{\kappa_2}_{EE} = \sqrt{\left. \frac{r_i a_{ji}}{r_j a_{ii}} \right|_i \left. \frac{r_i a_{jj}}{r_j a_{ij}} \right|_j}. \tag{S3.5}$$

This indicates that coexistence is stable (the right purple point in Fig. S2C).

Appendix S4: Asexual haploid coevolution model in Levin (1971)

We replicate Figure 5 of Levin (1971), where they considered competition dynamics between two species that have two genotypes as follows:

$$\frac{dn_i}{dt} = \lambda_i n_i \left(1 - \sum_{j=1}^{4} a_{ij} n_j \right), \quad i = 1,2,3,4, \tag{S4.1}$$

where λ_i is the intrinsic growth rate, a_{ij} is the inter-genotypic competition coefficient, $N_1 = n_1 + n_2$ is the population density of species 1, $N_2 = n_3 + n_4$ is the population density of species 2, $p_1 = n_1/N_1$ is the allele frequency of species 1, and $p_2 = n_3/N_2$ is the allele frequency of species 2. When the four genotypes have the same λ_i, the dynamics of population densities and allele frequencies can be represented by

$$\frac{dN_i}{dt} = r_i N_i \left(1 - \sum_{j=1}^{4} \alpha_{ij} N_j \right), \quad i = 1,2,$$

$$\frac{dp_1}{dt} = p_1 (1 - p_1) \left(\frac{1}{n_1} \frac{dn_1}{dt} - \frac{1}{n_2} \frac{dn_2}{dt} \right), \tag{S4.2}$$

$$\frac{dp_2}{dt} = p_2 (1 - p_2) \left(\frac{1}{n_3} \frac{dn_3}{dt} - \frac{1}{n_4} \frac{dn_4}{dt} \right),$$

where $r_i = \lambda_i$ and the intraspecific and interspecific competition coefficients are represented by

$$\alpha_{11} = a_{11} p_1^2 + \left(a_{12} + a_{21} \right) p_1 (1 - p_1) + a_{22} (1 - p_1)^2,$$

$$\alpha_{12} = p_1 \left[a_{13} p_2 + a_{14} (1 - p_2) \right] + (1 - p_1) \left[a_{23} p_2 + a_{24} (1 - p_2) \right],$$

$$\alpha_{21} = p_2 \left[a_{31} p_1 + a_{32} (1 - p_1) \right] + (1 - p_2) \left[a_{41} p_1 + a_{42} (1 - p_1) \right], \tag{S4.3}$$

$$\alpha_{22} = a_{33} p_2^2 + \left(a_{34} + a_{43} \right) p_2 (1 - p_2) + a_{44} (1 - p_2)^2.$$

In the parameter values of Figure 5 (see Table 2) in Levin (1971),

$$\begin{pmatrix} a_{11} & a_{12} & a_{13} & a_{14} \\ a_{21} & a_{22} & a_{23} & a_{24} \\ a_{31} & a_{32} & a_{33} & a_{34} \\ a_{41} & a_{42} & a_{43} & a_{44} \end{pmatrix} = \begin{pmatrix} 1 & 0.5 & 1.25 & 1.25 \\ 1.5 & 1 & 0.75 & 0.75 \\ 1.25 & 1.25 & 1 & 0.5 \\ 0.75 & 0.75 & 1.5 & 1 \end{pmatrix}, \quad (S4.4)$$

there is an intransitive competition relationship where n_1 beats n_2, n_2 beats n_3, n_3 beats n_4, and n_4 beats n_1 (Fig. S3A). In addition, n_2 and n_4 stably coexist but n_1 and n_3 show priority effect (Fig. S3A). The eco-evolutionary niche and competitive ability differences are:

$$\rho_{EE} = \sqrt{\frac{a_{41}a_{23}}{a_{11}a_{33}}},$$

$$\frac{\kappa_1}{\kappa_2}_{EE} = \sqrt{\frac{a_{33}a_{41}}{a_{11}a_{23}}}. \quad (S4.5)$$

and this is equivalent to the blue point (n_2 vs. n_4) in this case (Fig. S3B). Numerical simulations show that dynamics depend on initial conditions: when the allele frequencies are 0.5, there are cyclic dynamics (Fig. S3D) as predicted by Pimentel et al. (1965). When the initial condition is asymmetric in allele frequencies, the dynamics are either attracted to a stable equilibrium where n_2 and n_4 are dominant (i.e., p_1 and p_2 are low: Fig. S3E) or show seemingly heteroclinic cycles (Fig. S3C). Either way, they show the similar trade-off between α_{12} and α_{21} as the neighbor-dependent selection model of Vasseur et al. (2011).

Appendix S5: Coevolution model of character displacement in Pastore et al. (2021)

We replicate results of Pastore et al. (2021), where they considered eco-evolutionary dynamics between two species based on Barabás and D'Andrea (2016):

$$\frac{dN_i}{dt} = N_i\left(b_i - \sum_{j=1}^{2}\alpha_{ij}N_j\right),$$
$$\frac{d\mu_i}{dt} = h_i^2\left(g_i - \sum_{j=1}^{2}\beta_{ij}N_j\right),$$

(S5.1)

and

$$b_i = K_i - \frac{\mu_i^2 + \sigma^2}{\theta^2},$$

$$\alpha_{ij} = \sqrt{\frac{\omega^2}{\omega^2 + 4\sigma^2}}\exp\left[-\frac{(\mu_i - \mu_j)^2}{\omega^2 + 4\sigma^2}\right],$$

$$g_i = -\frac{2\mu_i\sigma^2}{\theta^2},$$

$$\beta_{ij} = \frac{-2\omega\sigma^2(\mu_i - \mu_j)}{(\omega^2 + 4\sigma^2)^{\frac{3}{2}}}\exp\left[-\frac{(\mu_i - \mu_j)^2}{\omega^2 + 4\sigma^2}\right],$$

(S5.2)

where N_i is the population density, μ_i is the mean trait, h_i^2 is the trait heritability, K_i is intrinsic population growth potential, σ is phenotypic standard deviation (assuming that the two species have the same phenotypic variance), θ is the environmental breadth, and ω is the competition width ($i = 1, 2$). The niche and competitive ability differences are

$$\rho = \exp\left[-\frac{(\mu_1 - \mu_2)}{\omega^2 + 4\sigma^2}\right],$$

$$\frac{\kappa_1}{\kappa_2} = \frac{K_1\theta^2 - \mu_1^2 - \sigma^2}{K_2\theta^2 - \mu_2^2 - \sigma^2}.$$

(S5.3)

11

This is similar to the classical character displacement, as the eco-evolutionary dynamics tends to increase niche difference (Fig. S4A) with a positive correlation between interspecific competition coefficients unlike other models considered in this study. When stable coexistence is possible (Fig. S4B-C), the eco-evolutionary niche and competitive ability differences (the gray point in Fig. S4A) do not indicate stable coexistence, in contrast to the value of the two metrics realized in simulations (the black point in Fig. S4A). As explained in the main text, this makes sense because at a stable equilibrium, the trait values are those that are optimal under a mixed species assemblage, which are not the values at the invasion condition endpoints.

References

Abrams, P. A. 2001. Modelling the adaptive dynamics of traits involved in inter- and intraspecific interactions: An assessment of three methods. Ecology Letters **4**:166-175.

Barabás, G., and R. D'Andrea. 2016. The effect of intraspecific variation and heritability on community pattern and robustness. Ecology Letters **19**:977-986.

Levin, B. R. 1971. The operation of selection in situations of interspecific competition. Evolution **25**:249-264.

Mougi, A. 2013. Allelopathic adaptation can cause competitive coexistence. Theoretical Ecology **6**:165-171.

Pastore, A. I., G. Barabás, M. D. Bimler, M. M. Mayfield, and T. E. Miller. 2021. The evolution of niche overlap and competitive differences. Nature Ecology & Evolution **5**:330–337.

Pimentel, D., E. H. Feinberg, P. W. Wood, and J. T. Hayes. 1965. Selection, spatial distribution, and the coexistence of competing fly species. The American Naturalist **99**:97-109.

Vasseur, D. A., P. Amarasekare, V. H. W. Rudolf, and J. M. Levine. 2011. Eco-evolutionary dynamics enable coexistence via neighbor-dependent selection. The American Naturalist **178**:E96-E109.
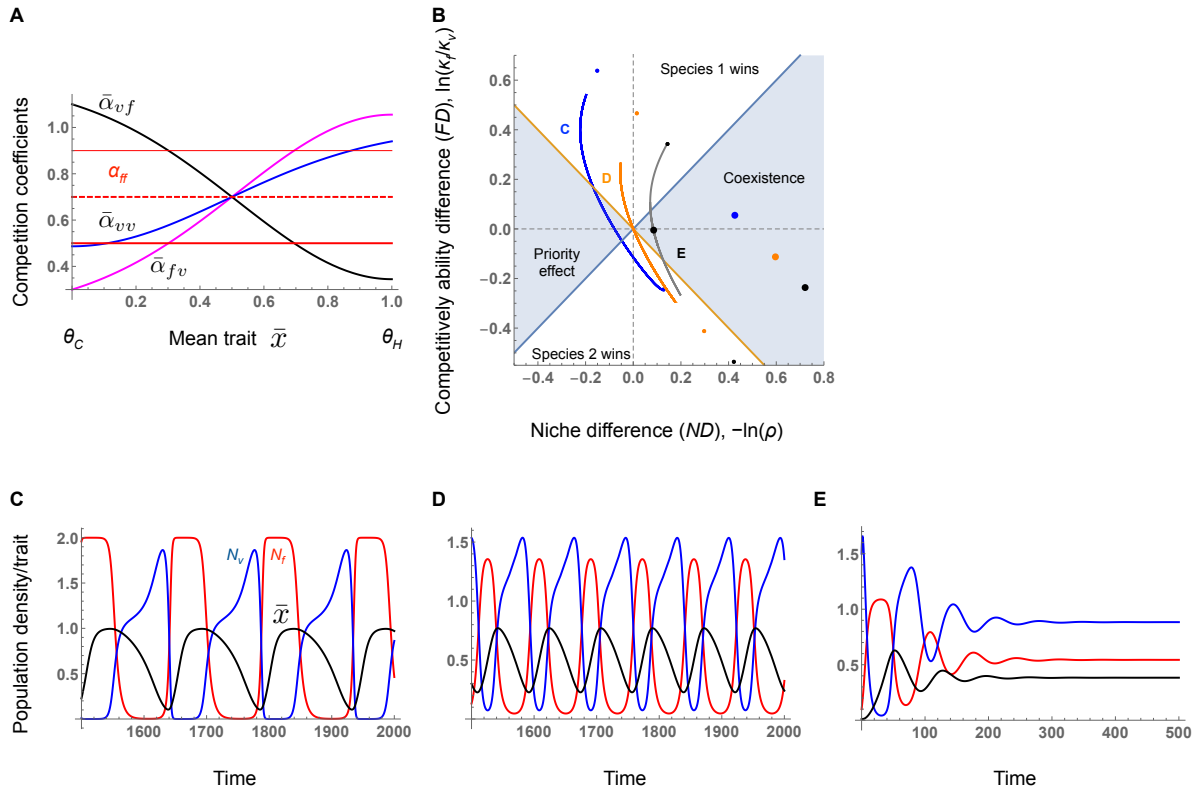
Figure S1 | Eco-evolutionary dynamics in Vasseur et al. (2011). A, The effects of the mean trait value on intraspecific and interspecific competition coefficients. Red thin, dashed, and thick horizontal lines represent $\alpha_{ff} = 0.9$, 0.7, and 0.5. **B**, Niche difference and competitive ability difference. The blue and orange curves labeled C and D represent trajectories of limit cycles in simulations in Fig. S1C-D. The black point labeled E is a stable equilibrium in Fig. S1E and the gray curve is a transient to the equilibrium. The top and bottom points are extreme values (when the trait value is θ_H or θ_C) while the larger points to the right represent the eco-evolutionary niche and competitive ability difference (Eq. S2.5). **C-E**, Simulation results with $\alpha_{ff} = 0.9$ (C), 0.7 (D), and 0.5 (E). Other parameter values are $r_v = r_f = 1$, $\theta_C = 0$, $\theta_H = 1$, $\tau = 0.412715$, $\sigma = 0.25$, $c_1 = \delta = 0.2$, and $H = 0.3$. See Appendix S2 for parameter explanations.
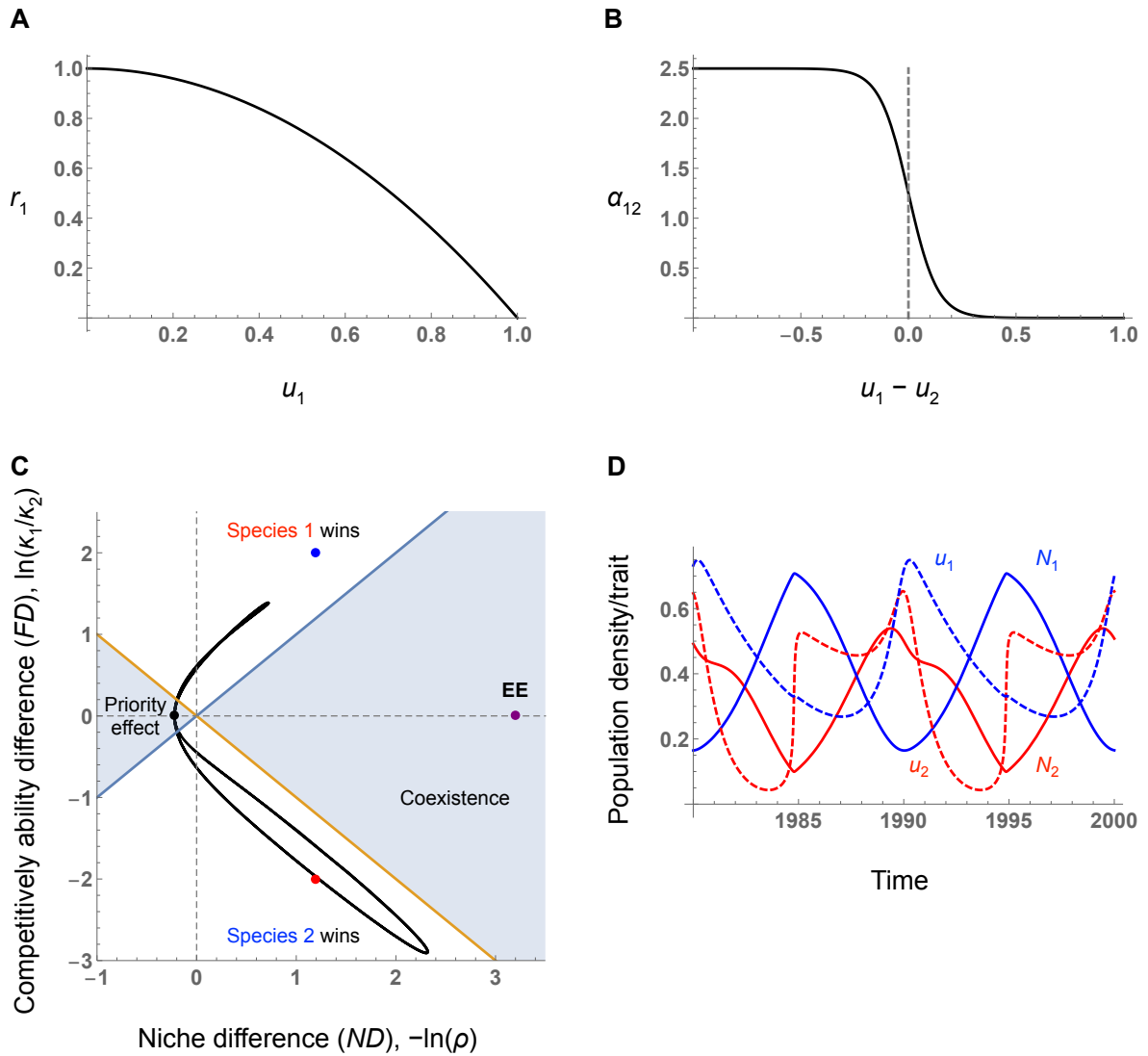
Figure S2 | Eco-evolutionary dynamics in Mougi (2013). A-B, Effects of the trait value on the per-capita growth rate (A) and the effect of the trait difference on the interspecific competition coefficient (B). **C**, Niche difference and competitive ability difference. Black trajectories show simulation results in D. **D**, The simulation result of Fig. 1c in Mougi (2013). Parameter values are $r_0 = 1$, $\alpha_0 = 2.5$, $\rho_i = 2$, $\theta = 15$, $G_1 = 0.5$, and $G_2 = 0.1$. Note that $G_i = 0.005$ in Fig. 4. See Appendix S3 for parameter explanations.
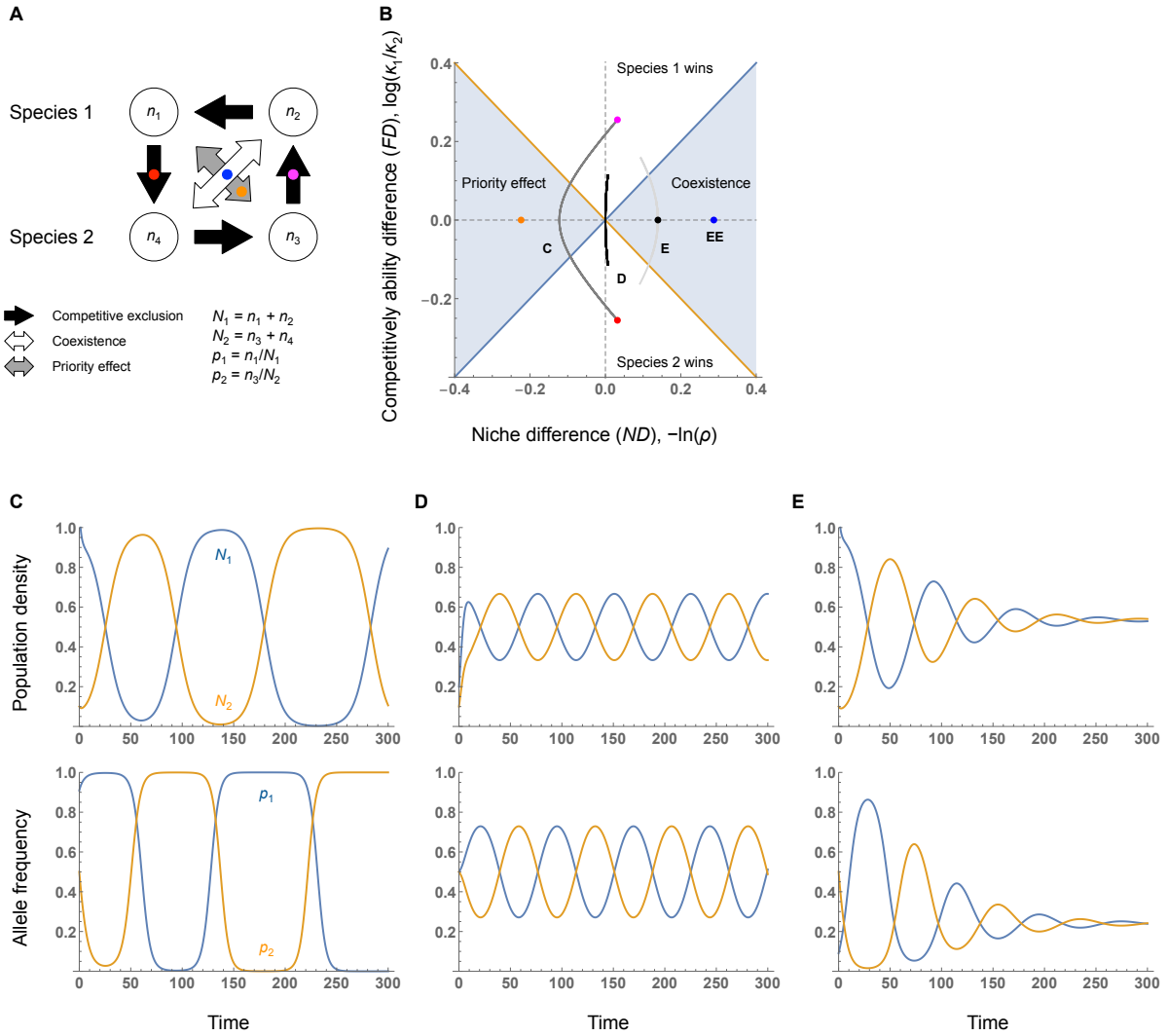
Figure S3 | Eco-evolutionary dynamics in Levin (1971). A, Competition relationships
between genotype i, n_i (i = 1-4). Black, white, and gray arrows between genotypes represent
competition outcomes between two genotypes based on parameter values of Equation S4.4:
unidirectional black arrows indicate competitive exclusion (e.g., genotype 1 excludes
genotype 2 because a_{12} = 0.5 and a_{21} = 1.5), a white arrow indicates stable coexistence, and a
gray arrow represents priority effect. **B**, Niche difference and competitive ability difference.
Blue, red, orange, and magenta points represent niche and competitive ability differences in
competition between two genotypes shown in A (according to the parameter values of
Equation S4.4). Gray, black, and light gray curves show simulation results in C-E. **C-E**,

16

Simulation results with different initial conditions: $(n_1, n_2, n_3, n_4) = (0.1, 0.1, 0.05, 0.05)$ (C), $(1, 0.1, 0.05, 0.05)$ (D), and $(0.1, 1, 0.05, 0.05)$ (E). As shown in A, $N_1 = n_1 + n_2$, $N_2 = n_3 + n_4$, $p_1 = n_1/N_1$, and $p_2 = n_3/N_2$. Here $r_i = 0.5$. See Appendix S4 for parameter explanations.

A, Niche difference and competitive ability difference. **B**, Population density vs Time. **C**, Mean trait vs Time.
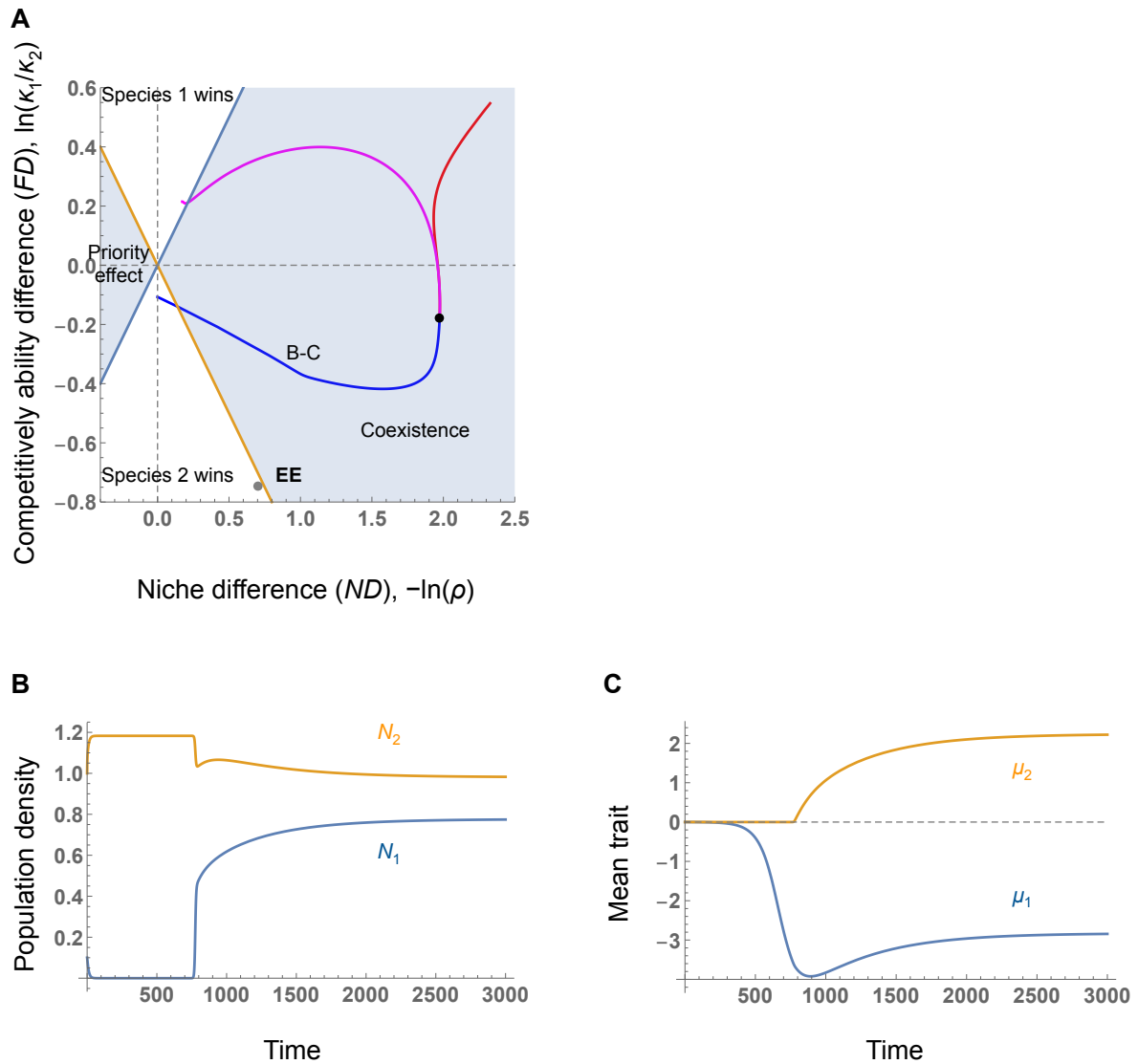
Figure S4 | Eco-evolutionary dynamics in Pastore et al. (2021). A, Niche difference and

competitive ability difference. Red, blue, and magenta trajectories show simulation results

with the initial conditions, $(N_1(0), N_2(0), \mu_1(0), \mu_2(0)) = (0.1, 1, 0, 5.5)$, $(0.1, 1, 0, 0.001)$, and

$(0.1, 1, 4, 5.5)$. The gray point represents eco-evolutionary niche and competitive ability

differences. **B-C**, The simulation results shown by the blue curve in A. Parameter values are

$K_1 = 0.9$, $K_2 = 1$, $\sigma = 1$, $h^2 = 0.1$, $\omega = 3$, and $\theta = 8$. See Appendix S5 for parameter

explanations.